

## Corrosion resistance of electroless deposited Ni-P coatings on polymer (ABS) substrate

V. Chakarova\*, M. Georgieva, M. Petrova

*Institute of Physical Chemistry, Bulgarian Academy of Sciences,  
Acad. G. Bonchev Str., Bl. 11, 1113 Sofia, Bulgaria*

Submitted on July 26, 2016; Revised on October 31, 2016

Nickel-phosphorus and composite nickel-phosphorus coatings with dispersed diamond particles (with 14-20  $\mu\text{m}$  particles size) are produced by electroless deposition onto an Acrylonitrile-Butadiene-Styrene (ABS) substrate. The influence of deposition time and solution acidity on the deposition rate, phosphorus content and microhardness of the obtained coatings is investigated. The corrosion resistance of coatings deposited at two different pH values of the electrolyte is evaluated by Neutral Salt Spray (NSS) tests and the potentiodynamic investigations are carried out in a model corrosive medium 0.5 M  $\text{Na}_2\text{SO}_4$  solution with pH 5.9. Scanning electron microscopy (SEM) is employed to examine the morphology of the deposits before and after the corrosion resistance test, and the changes in elemental composition of the coatings are determined by X-ray diffraction analysis (XRD). The results of these tests and analyses show that incorporation of diamond particles in the Ni-P coatings is advantageous for forming better passive films with improved corrosion resistance.

**Keywords:** electroless deposition, composite coatings Ni-P, diamond particles, microhardness, corrosion resistance, SEM, XRD

### INTRODUCTION

The electroless coatings are mainly applied for wear resistance and corrosion resistance operations [1-6]. The properties of the electroless nickel-phosphorus alloy (Ni-P) strongly depend on the phosphorus content [2]. The P content can be changed by varying certain conditions of plating, such as composition and pH of the plating bath used. Typically, higher pH values yield lower phosphorus content in the deposit, while lower ranges produce high phosphorus deposits. Several studies have shown that Ni-P alloys provide good anticorrosive coatings. In general, electroless Ni-P is a barrier coating, protecting the substrate by sealing it off from the corrosive environments, rather than by sacrificial action [7]. The high resistance was a result of the amorphous nature and passivity of the Ni-P deposits. The corrosion resistance of electroless Ni-P coatings is a function of composition. Most deposits are naturally passive and very resistant to corrosion attack in most environments. Their degree of passivity and corrosion resistance, however, is greatly affected by their phosphorus content. Alloys containing more than 10 mass % P are more resistant to attack than those with lower phosphorus content in neutral or acidic environments. Alloys containing low phosphorus content (3 to 4 mass % P) are more resistant to strong alkaline environment than high phosphorus deposits [3]. It is believed that anodic

dissolution is accompanied by preferred dissolution of nickel and phosphorus enrichment to the surface [8].

To further enhance the properties of the Ni-P deposits, second phase particles have been introduced into the Ni-P matrix. The characteristics of Ni-P composite coatings depend on phosphorus content of the Ni-P matrix and on certain properties of the particles such as type, shape and size [9]. Incorporation of particles improves the mechanical and tribological properties of the Ni-P deposits [1, 9-12], but there is a disagreement among researchers regarding the corrosion resistance of the electroless composite coatings [9, 13].

The choice of appropriate particles is very important for the simple production of functional composite coatings with specific characteristics. A great number of studies have been devoted to the production of Ni-P composite coatings with incorporated diamond particles of various sizes [9, 13-20]. The obtained results have demonstrated that Ni-P/nano-diamond composite coatings exhibit better performances than Ni-P coatings and also optimum deposition of Ni-P/nano-diamond shows more desirable characteristics of corrosion properties rather than as deposited Ni-P coatings [9, 13, 15, 17].

The aim of the present work is to study the corrosion behaviour of Ni-P and composite Ni-P coatings with dispersed 14-20  $\mu\text{m}$  diamond particles. The coatings are deposited onto acrylonitrile-butadiene-styrene (ABS) samples to eliminate the influence of the substrate.

---

\* To whom all correspondence should be sent:

E-mail: [vchakarova@ipc.bas.bg](mailto:vchakarova@ipc.bas.bg)

**Table 1.** Technological scheme of the processing samples of ABS

Operation	Substance	Concentration, g.l <sup>-1</sup>	Time, min	Temperature, °C
Etching	CrO <sub>3</sub>	367	15	65
	H <sub>2</sub> SO <sub>4</sub>	253		
Pre-activation	HCl	3M	3	20
Activation	PdCl <sub>2</sub>	0.8	5	20
Acceleration	NaOH	1M	5	20
Chemical metalization	In Table 2			

**Table 2.** Chemical compositions and operating conditions of the plating bath

Substance	Concentration
NiSO <sub>4</sub> .7H <sub>2</sub> O, g.l <sup>-1</sup>	25
NaH <sub>2</sub> PO <sub>2</sub> .H <sub>2</sub> O, g.l <sup>-1</sup>	22
CH <sub>3</sub> COONa, g.l <sup>-1</sup>	20
Lactic acid, g.l <sup>-1</sup>	20
Stabilizer 2 (a commercial product of TU-Sofia), mg.l <sup>-1</sup>	1
NaLS, g.l <sup>-1</sup>	0.01
<b>Operating condition</b>	
pH	4.6 - 4.8
Temperature, (°C)	82

## EXPERIMENTAL

The nickel coatings were deposited onto samples of ABS (Novodur PM/2C, Bayer, Germany) with a working area of 0.2 dm<sup>2</sup>. The employed technological scheme is presented in Table 1.

The composition of the Ni-P bath is presented in Table 2.

Diamond particles with particle size of 14-20 μm (D) were added to the solution for chemical deposition in concentration of 5 g.l<sup>-1</sup>. The conditions of electroless deposition of Ni-P and composite Ni-P (Ni-P/D) coatings are described in earlier papers [20, 21].

The deposition rate, expressed in terms of the amount of deposited nickel, resp. the relative thickness of the obtained coating ( $\delta$ , μm), was determined gravimetrically as the difference in sample mass before and after deposition of the composite coating:

$$\delta = \Delta m \cdot 10^4 / \rho \cdot S, [\mu\text{m}]$$

where,  $\rho$  - density of nickel in [g.cm<sup>-3</sup>]; S - working area in [cm<sup>2</sup>];  $\Delta m$  - mass of the deposited coating.

The coatings were tested for corrosion resistance employing a Neutral Salt Spray test (NSS) (5% NaCl, pH 6.6-7.2) (VSN 1000, Vötsch Industrietechnik GmbH), comprising three test cycles of 24 hours each. The corrosion damage was determined gravimetrically based on mass loss. The microhardness of the coatings was measured by the Vickers method at a load of 50 p (Durimet, Ernst Leitz GmbH).

Open circuit potential (OCP)-time transients were plotted in 0.5 M Na<sub>2</sub>SO<sub>4</sub> solution with pH 5.9. Potentiodynamic polarization was applied to study

the anodic dissolution of the coatings. A potential scan rate of 1 mV.s<sup>-1</sup> was applied by starting from a potential 250 mV more cathodic than the OCP and scanned in anodic direction. The investigations were performed in a three-electrode cell with a volume of 50 ml, Hg/Hg<sub>2</sub>SO<sub>4</sub> reference electrode, working electrode with surface area of 0.2 cm<sup>2</sup> and Pt counter electrode. All electrochemical experiments were carried out using a potentiostat/galvanostat model 263A (EG&G Princeton Applied Research, USA) and SoftCorr II software. The polarization resistance ( $R_p$ ) and the corrosion current density ( $j_{\text{corr}}$ ) were calculated from data collected during the potentiodynamic polarization.

The structures of the produced thin films were characterized by X-ray diffraction (XRD) using a PANalytical Empyrean equipped with a multichannel detector (Pixel 3D) using (Cu K $\alpha$  45 kV-40 mA) radiation in the 10–100 2 $\theta$  range, with a scan step of 0.01 for 24 s.

The morphology and structure of the obtained coatings, as well as the distribution of the dispersoid particles on their surface, were examined by a Metallographic Microscope (AMPLIVAL<sup>®</sup> pol u Carl Zeiss JENA, Germany) and by Scanning Electron Microscopy (SEM) (JEOL JSM 733, Japan). The average amount of co-deposited particles per square centimeter (N.cm<sup>-2</sup>) was determined based on the number of particles, counted on the surface of the composite coating by SEM (the counting was done in three arbitrarily chosen zones at a magnification 200x). Energy Dispersive Spectroscopy (EDS/INCA) was used to determine the elemental chemical composition of the coatings.

## RESULTS AND DISCUSSION

### Characterization of Ni-P and Ni-P/D coatings

Hypophosphite reduces nickel ions at electrolyte pH values higher than 3. The rate of hypophosphite oxidation and of nickel deposition increases with increase of solution pH, but at pH values above 5.5, the electrolyte stability decreases. Therefore, two pH values were selected within the range 3.0-5.5 for electroless deposition of Ni-P coatings and investigation of the deposition rate and microhardness tests of the obtained coatings. The obtained results are summarized in Table 3.

For the same deposition time, the thickness of the coating deposited in electrolyte with pH 3.8 is twice smaller than that obtained at pH 4.8. With increase of the electrolyte pH the P content of the coating decreases, but its microhardness increases.

**Table 3.** Influence of the pH of the electrolyte on the thickness and microhardness of Ni-P coatings on  $\tau = 30$  min.

pH	3.8	4.8
$\delta$ , ( $\mu\text{m}$ )	4.8	10.2
HV <sub>50</sub> , (kg.mm <sup>-2</sup> )	275	640
P, (mass %)	14.9	6.4

The significantly lower microhardness of the coating deposited at pH 3.8 is not related to its thickness. Similar microhardness values were also measured for samples with a thickness of 30-35  $\mu\text{m}$ . These results made us initiate deposition tests in the electrolyte with pH 4.8 but for different deposition times. It was established that the microhardness of the coatings increased but slightly with increase of coating thickness (Fig. 1).

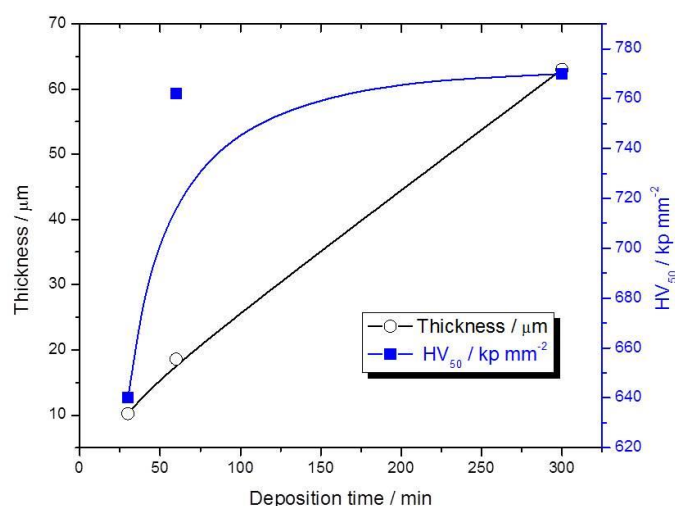


**Fig. 1.** Influence of deposition time on the thickness and microhardness of Ni-P coatings. Electrolyte pH 4.8

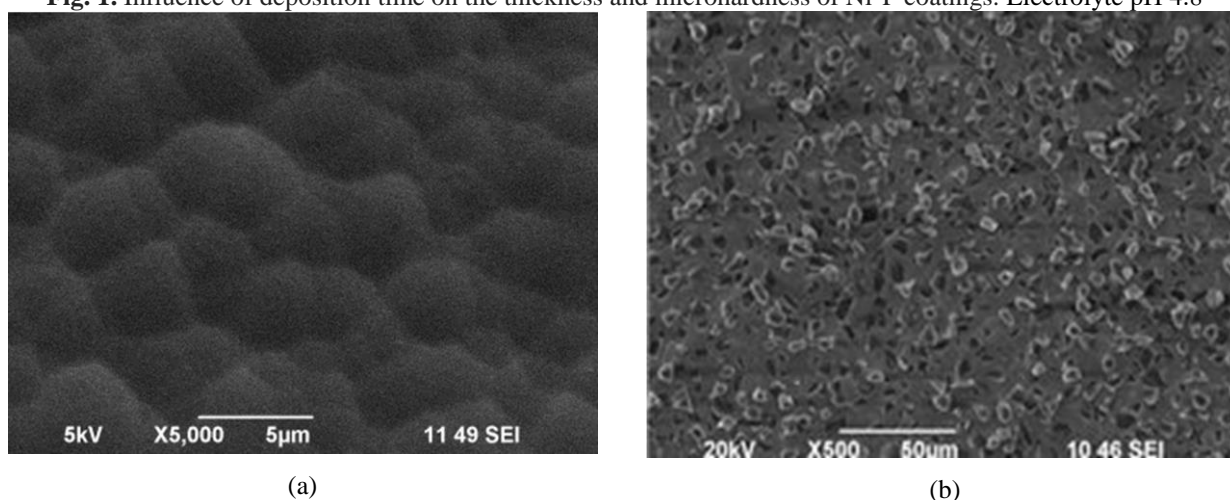


**Fig. 2.** SEM image of: a) Ni-P coating; b) Ni-P/D coating,  $\tau = 30$  min.

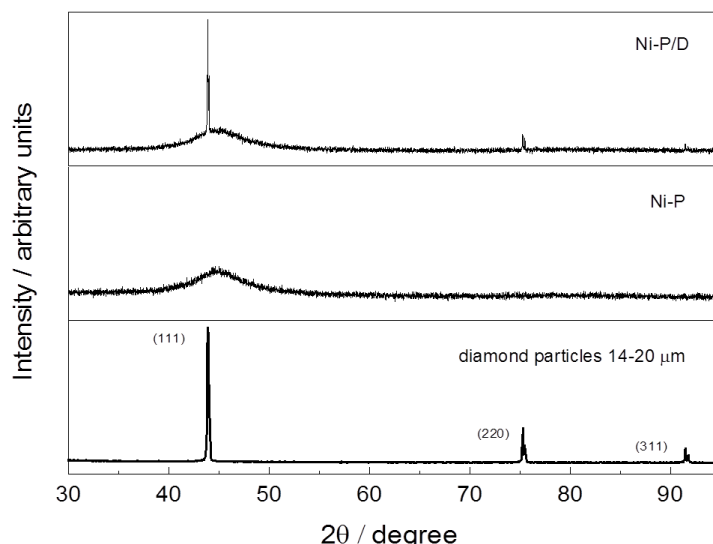


**Fig. 3.** XRD pattern of as deposited Ni-P, Ni-P/D coatings and diamond particles with size of 14-20  $\mu\text{m}$ .

Composite coatings were deposited with addition of diamond particles to the solution for chemical deposition in concentration of 5  $\text{g.l}^{-1}$ . The number of incorporated particles is of the order of 150 000 – 200 000  $\text{N.cm}^{-2}$ . Figure 2 shows the morphology of such a coating.

The microhardness tests of the Ni-P/D coatings were not conducted, because of the great number and size of incorporated particles.

#### *XRD analysis of Ni-P and Ni-P/D coatings*

Figure 3 shows the XRD patterns of the obtained Ni-P and Ni-P/D coatings. Both coatings have amorphous structure. For comparison, the X-ray diffractogram of diamond particles is also presented and it indicates that the reflexes for the composite coating come from the incorporated particles.

#### *Corrosion resistance tests of in a NSS chamber*

Three samples from each type of coatings were prepared for testing in the corrosion chamber. The samples were with sizes 5 X 10 cm. The thickness of the coatings was in the range of 20-25  $\mu\text{m}$ . The coatings were not evaluated visually or by optical methods because there were no visible signs of corrosion damage on their surface. The mass loss values for the respective coatings after the NSS test are presented in Table 4.

**Table 4.** Weight loss for the Ni-P and Ni-P/D coatings after 72 hours in a neutral salt spray chamber.

pH	Weight loss, mg	
	Ni-P	Ni-P/D
3.8	3.8	10.1
4.8	3.3	8.3

All coatings lose mass with prolonged time of stay in the chamber, the measured mass loss being more substantial for the composite coatings with incorporated particles. This is, probably, due to

localized corrosion around the particles, which leads eventually to their shedding off the coating. Figure 4 shows the morphology of the specimens after the NSS test.

#### *Electrochemical corrosion performance of Ni-P and Ni-P/D coatings*

Figure 5 presents the potentiodynamic polarization curves of dissolution of the Ni-P and Ni-P/D coatings in model corrosive environment: 0.5 M  $\text{Na}_2\text{SO}_4$ , pH 5.9. The indifferent substrate used allowed plotting of polarization curves up to potentials sufficiently positive for oxygen evolution. On grounds of the obtained results it can be concluded that incorporation of diamond particles in the coating improves its corrosion behavior as compared to that of the deposit on pure Ni-P matrix. The corrosion potential of the composite coating deposited at pH 3.8 shifts to more positive values and the corrosion rate is much lower within a wide potential range. A plateau appears at about -600 mV which, according to literature data, is related to saturation of the surface layer with phosphorus resulting in impeded coating dissolution [8]. The curve for the composite coating deposited at pH 4.8 features an even broader passivation plateau and hence lower corrosion rate.

The corrosion potential ( $E_{\text{corr}}$ ), corrosion current density ( $j_{\text{corr}}$ ) and polarization resistance ( $R_p$ ) of the different coatings, determined from the respective potentiodynamic polarization curves, are presented in Table 5.

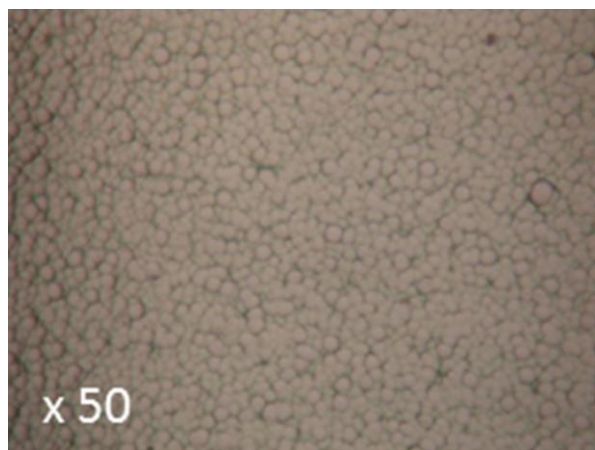
Passivation of the remaining coating layer is recorded at about +600 mV in the curves for all samples. On completion of the potentiodynamic measurements, the remaining coating layer on the surface of all specimens has an average thickness of the order of 1  $\mu\text{m}$  (Table 6).

**Table 5.** Corrosion characteristics of Ni-P and Ni-P/D coatings deposited at pH 4.8 in model corrosive environment.

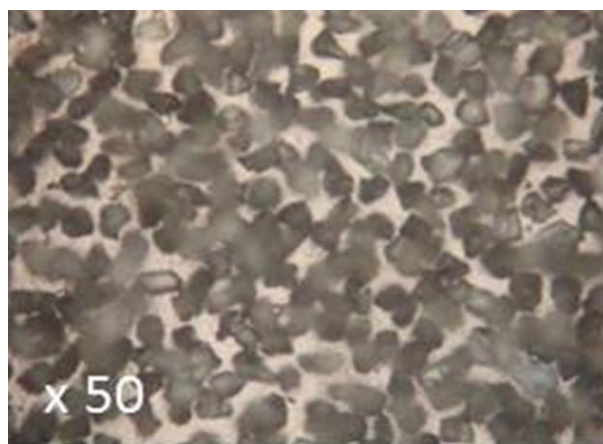
	$E_{corr}$ , (mV)	$j_{corr}$ , ( $\mu\text{A}\cdot\text{cm}^{-2}$ )	$R_p$ , ( $\text{k}\Omega\cdot\text{cm}^2$ )
Ni-P	-870	2.1	24
Ni-P/D	-890	1.0	35

**Table 6.** Influence of electrochemical treatment according Fig. 5 on the thickness of the Ni-P and Ni-P/D coatings.

	$\delta$ , ( $\mu\text{m}$ )	
	Ni-P	Ni-P/D
Before potentiodynamic polarization	12.5	9.2
After potentiodynamic polarization	1.1	1.9

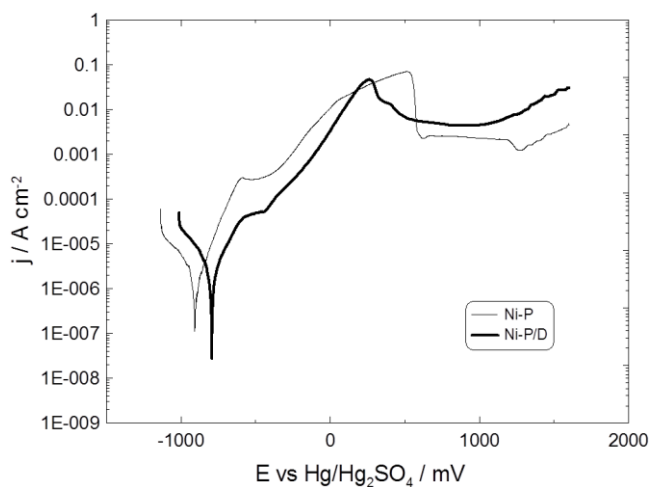


(a)

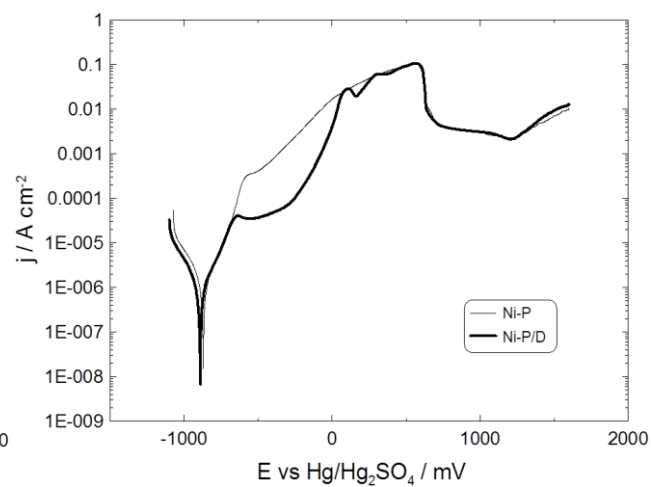


(b)

**Fig. 4.** Optical imaging of coatings after 72 hours in neutral salt spray chamber: a) Ni-P; b) Ni-P/D.



(a)



(b)

**Fig. 5.** Potentiodynamic polarization curves in model corrosive environment of Ni-P and Ni-P/D coatings deposited in electrolyte with a pH: a) 3.8; b) 4.8.

The SEM images in Fig. 6 compare the surface of the coatings without (Fig. 6a) and with (Fig. 6b) incorporated diamond particles after the potentiodynamic tests. The composite Ni-P/D coating dissolves more uniformly than the Ni-P

coating. The latter features general thinning in the central work area and dissolves completely in the peripheral zones (Fig. 6a).



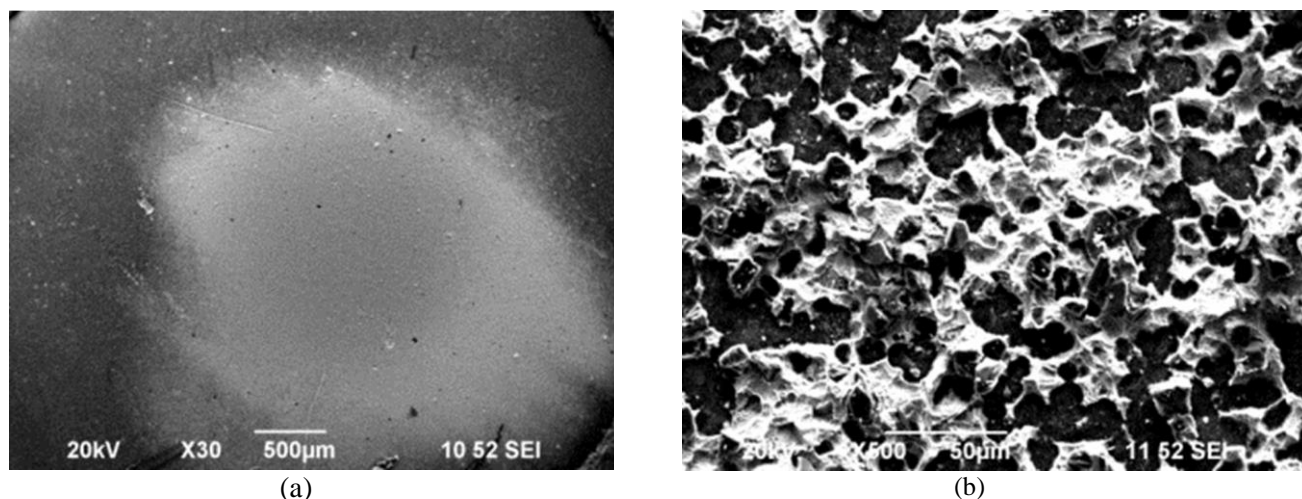


**Fig. 6.** SEM images of coatings (deposited at pH 4.8) after anodic potentiodynamic dissolution: a) Ni-P; b) Ni-P/D.

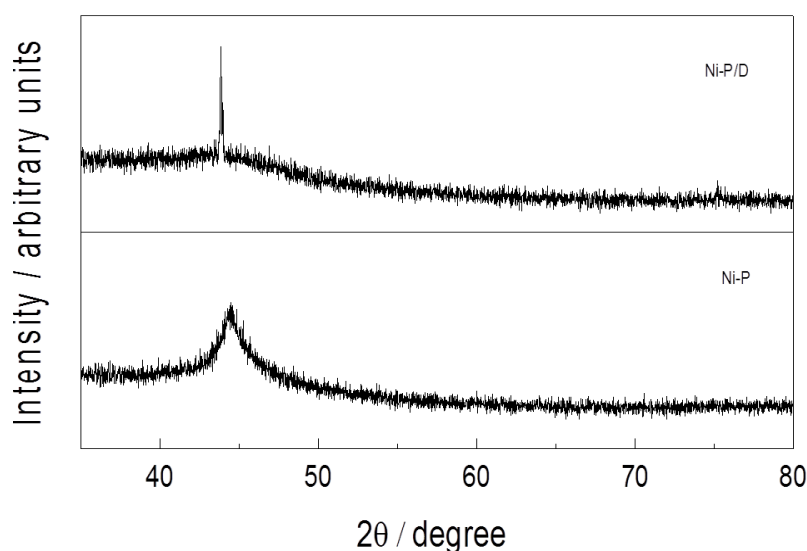


**Fig. 7.** XRD pattern of Ni-P and Ni-P/D coatings (deposited at pH 4.8) after anodic potentiodynamic dissolution according Fig. 5.

The XRD spectra show that both the Ni-P and Ni-P/D coatings have preserved their amorphous structure after the electrochemical test (Fig. 7). The results of the X-ray microanalysis indicate that the percent P content is preserved, too. The recorded reflexes evidence the incorporated particles in the coatings, irrespective of their low thickness, which is an indication of their good adhesion to the matrix.

### CONCLUSIONS

Ni-P and composite Ni-P/D coatings with diamond particles sized 14-20  $\mu\text{m}$  are produced by electroless deposition in electrolytes with two pH values: 3.8 and 4.8.

With increase of the electrolyte pH the thickness and microhardness of the Ni-P coatings increase, but the P content decreases.

A slight increase in microhardness of the Ni-P coatings with deposition time is observed when they are deposited at electrolyte pH 4.8.

With increase of the time of stay in the neutral salt spray chamber the coatings lose mass, more notably when they contain incorporated diamond particles.

On anodic polarization in sulfate medium up to the potential of oxygen evolution, the coatings do not dissolve completely. The composite Ni-P/D coatings dissolve more uniformly than the Ni-P deposits, they preserve their amorphous structure and exhibit lower corrosion rate.

### REFERENCES

1. M. M. Mirza, E. Rasu, A. Desilva, *Amer. Chem. Sci. J.*, **13**, 1 (2016).
2. C.A. Loto, *Silicon*, **8**, 177 (2016).

3. K. Hari Krishnan, S. John, K. N. Srinivasan, J. Praveen, M. Ganesan, P.M. Kavimani, *Metall. Mater. Trans.*, **37**, 1917 (2006).
4. C. Larson, J. R. Smith, G. J. Armstrong, *Trans. Inst. Metal Finishing*, **3**, 120 (2013).
5. B. W. Zhang, S. Z. Liao, H. W. Xie, H. Zhang, *Trans. Inst. Metal Finishing*, **6**, 310 (2013).
6. X. Shu, Y. Wang, J. Peng, P. Yan, B. Yan, X. Fang, Y. Xu, *Int. J. Electrochem. Sci.*, **10**, 1261 (2015).
7. T. Rabizadeh, S. Reza Allahkaram, *Mater. Design*, **32**, 133 (2011).
8. I. V. Petukhov, N. A. Medvedeva, I. R. Subakova, V. I. Kichigin, *Protctn Metals & Phys. Chem. Surfaces*, **50**, 875 (2014).
9. J. N. Balaraju, T. S. N. Sankara Narayanan, S. K. Seshadri, *Journal of Applied Electrochemistry*, **33** (2003) 807–816.
10. A. Sharma, A. K. Singh, *J. Materials Eng. Performance*, **22**, 176 (2013).
11. M. Islam, M. R. Azhar, N. Fredj, T. D. Burleigh, O. R. Oloyede, A. A. Almajid, S. I. Shah, *Surface Coatings Technol.*, **261**, 141 (2015).
12. P. Makkar, R.C. Agarwala, V. Agarwala, *J Mater Sci*, **50**, 2813 (2015).
13. H. Xu, Z. Yang, M.-Ke Li, Y.-Li Shi, Y. Huang, H.-Lin Li, *Surface Coatings Technol.*, **191**, 161 (2005).
14. V.V.N. Reddy, B. Ramamoorthy, P. Kesavan Nair, *Wear*, **239**, 111 (2000).
15. Y. L. Shi, Z. Yang, H. Hu, M. K. Li, H. L. Li, *J. Materials Sci.*, **39**, 5809 (2004).
16. X.T. Huang, G.Y. Cai, *Appl. Mech. Materials*, **26-28**, 843 (2010).
17. H. Mazaheri, S. Reza Allahkaram, *Appl. Surface Sci.*, **258**, 4574 (2012)..
18. S.R. Allahkaram, H. Mazaheri, *Iranian J. Materials Sci. Eng.*, **11**, 18 (2014).
19. C.K. Lee, C.L. Teng, A.H. Tan, C.Y. Yang, S.L. Lee, *Key Eng. Materials*, **656-657**, 51 (2015).
20. M. Petrova, M. Georgieva, V. Chakarova, E. Dobreva, *Arch. Metall. Mater.*, **61**, 493 (2016).
21. M. Georgieva, M. Petrova, V. Chakarova, *Bulg. Chem. Commun.*, **45**, 116 (2013).

## КОРОЗИОННА УСТОЙЧИВОСТ НА БЕЗТОКОВИ Ni-P ПОКРИТИЯ ПОЛУЧЕНИ ВЪРХУ ПОЛИМЕРНА ПОДЛОЖКА (ABS)

В. Чакърова, М. Георгиева, М. Петрова

*Институт по физикохимия - Българска академия на науките  
София, 1113, ул. „Акад. Г. Бончев”, бл.11  
секция „Електрохимия и корозия”*

Постъпила на 26 юли, 2016 г. коригирана на 31 октомври, 2016 г.

(Резюме)

По метода на безтоково отлагане са получени Ni-P и композитни Ni-P покрития с диамантени частици с размер 14-20  $\mu\text{m}$  върху подложка от акрилонитрил бутадиен стирол. Изследвано е влиянието на времето на отлагане и киселинността на разтвора върху скоростта на отлагане, съдържанието на фосфор и микротвърдостта на покритията. Корозионни изпитания на покрития, получени при две стойности на pH на електролита са проведени в камера за неутрална солена мъгла, а потенциодинамични криви са снети в моделна корозионна среда - 0.5M Na<sub>2</sub>SO<sub>4</sub> solution with pH 5.9. С помощта на сканираща електронна микроскопия е изследвана морфологията на покритията преди и след изпитанията, а чрез рентгенов микроанализ са определени измененията в елементния състав. Резултатите показват, че включването с на диамантени частици в Ni-P покритие се образуват пасивни филми с добра корозионна устойчивост.